BIOCHEMISTRY
including biophysical chemistry & molecular biology

Article

pubs.acs.org/biochemistry

Comparative Study of Two Chitin-Active and Two Cellulose-Active AA10-Type Lytic Polysaccharide Monooxygenases

Zarah Forsberg,[†] Åsmund Kjendseth Røhr,[‡] Sophanit Mekasha,[†] K. Kristoffer Andersson,[‡] Vincent G. H. Eijsink,[†] Gustav Vaaje-Kolstad,[†] and Morten Sørlie*[,†]

[†]Department of Chemistry, Biotechnology and Food Science, Norwegian University of Life Sciences, P.O. Box 5003, N-1432 Ås, Norway

[‡]Department of Biosciences, University of Oslo, P.O. Box 1066, Blindern, N-0316 Oslo, Norway

Supporting Information

ABSTRACT: Lytic polysaccharide monooxygenases (LPMOs), found in family 9 (previously GH61), family 10 (previously CBM33), and the newly discovered family 11 of auxiliary activities (AA) in the carbohydrate-active enzyme classification system, are copper-dependent enzymes that oxidize sp^3-carbons in recalcitrant polysaccharides such as chitin and cellulose in the presence of an external electron donor. In this study, we describe the activity of two AA10-type LPMOs whose activities have not been described before and we compare in total four different AA10-type LPMOs with the aim of finding possible correlations between their substrate specificities, sequences, and EPR signals. EPR spectra indicate that the electronic environment of the copper varies within the AA10 family even though amino acids directly interacting with the copper atom are identical in all four enzymes. This variation seems to be correlated to substrate specificity and is likely caused by sequence variation in areas that affect substrate binding geometry and/or by variation in a cluster of conserved aromatic residues likely involved in electron transfer. Interestingly, EPR signals for cellulose-active AA10 enzymes were similar to those previously observed for cellulose-active AA9 enzymes. Mutation of the conserved phenylalanine positioned in close proximity to the copper center in AA10-type LPMOs to Tyr (the corresponding residue in most AA9-type LPMOs) or Ala, led to complete or partial inactivation, respectively, while in both cases the ability to bind copper was maintained. Moreover, substrate binding affinity and degradation ability seemed hardly correlated, further emphasizing the crucial role of the active site configuration in determining LPMO functionality.

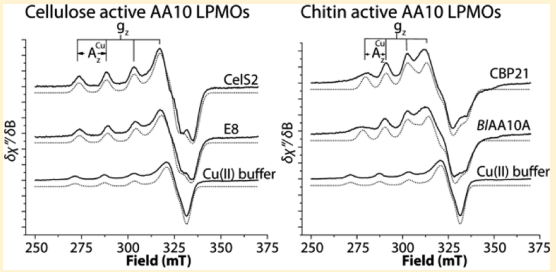

Lytic polysaccharide monooxygenases (LPMOs) make up a newly discovered group of carbohydrate-active enzymes, that as of 2013 are classified as auxiliary activities (AA) in the CAZy database.[1] Family AA9, previously classified as glycoside hydrolase family 61 (GH61), and family AA10, previously classified as carbohydrate binding module family 33 (CBM33), use an oxidative mechanism to cleave crystalline polysaccharides such as cellulose and chitin.[2−4] Recently, a new family (AA11) active on chitin that appears to have characteristics of both AA9 and AA10 has been discovered.[5] AA10-type proteins occur in all domains of life and are best known from work on bacterial and viral family members, which initially were believed to be chitin binding proteins lacking a catalytic function.[6,7] AA9-type proteins occur in fungi and were originally classified as glycoside hydrolases because of the observation of a low endo activity in cellulose degradation.[8,9] Most LPMO-containing organisms encode several LPMOs that are upregulated when different cellulose or chitin substrates are used as the sole carbon source, indicating that these enzymes are important for the organism's ability to degrade biomass.[10,11]

The first indications of AA10 enzyme activity were published in 2005 and 2008; chitin binding protein 21 (CBP21) from *Serratia marcescens* and E7 and E8 from *Thermobifida fusca*, respectively, were shown to enhance the enzymatic conversion of insoluble polysaccharides.[12,13] In 2010, Vaaje-Kolstad et al.[2] showed that CBP21 is an oxidative enzyme that introduces chain breaks into crystalline chitin in a reaction dependent on a divalent metal ion, an external electron donor, and molecular oxygen. Shortly afterward, it was shown that an AA10[3] as well as AA9-type LPMOs[4,14−16] could cleave and oxidize cellulosic substrates. After some initial confusion about the nature of the divalent metal ion, it has become clear that LPMOs are copper-dependent enzymes.[4,17] In addition to having different substrate specificities, LPMOs also differ in terms of their preference for the position of reaction. All AA10 enzymes described so far oxidize C1, whereas for AA9 enzymes, oxidation has been reported at C1 and C4 or C6.[4,15,16,18]

The CBP21 crystal structure was the first LPMO structure to be determined.[19] This AA10 enzyme has a small and globular structure with a flat binding surface that seems to be adapted to binding to crystalline parts of the chitin substrate primarily through polar interactions. The first AA9-type LPMO structure

Received: January 10, 2014
Revised: February 18, 2014
Published: February 21, 2014

   dx.doi.org/10.1021/bi5000433 | *Biochemistry* 2014, 53, 1647−1656

to be determined was that of Cel61B from *Hypocrea jecorina* (*Hj*AA9B, CAZy abbreviation).[20] AA9- and AA10-type LPMOs have no significant overall sequence identity but are structurally similar and contain a highly conserved metal binding site in their catalytic centers.[21,22] X-ray crystallography and EPR studies of AA9-type LPMOs have shown that these enzymes contain a type 2 copper binding site where the copper has six ligands. The four ligands in the equatorial plane include nitrogens from two fully conserved histidine side chains and the N-terminal amino group, together forming a T-shaped histidine brace; the fourth equatorial ligand is a water molecule coordinated by a conserved and functionally important glutamine.[4,9,21,22] The axial ligands are the hydroxyl group of a conserved tyrosine (i.e., most likely a tyrosinate) and another water molecule.[4] Available structural information for AA10-type LPMOs also shows or suggests a T-shaped coordination of the metal, but only involving the equatorial sites. The tyrosine residue in AA9-type LPMOs is replaced by phenylalanine in most AA10-type LPMOs; the glutamine coordinating the axial water is absent, and access to this axial site seems to be restricted by a side chain (most commonly an alanine residue).[21] Another dissimilarity between the two LPMO families concerns the N-terminal histidine, which tends to be methylated (Nε-Me) in AA9-type LPMOs expressed in their fungal hosts,[4,23] whereas such methylation has not been observed for AA10-type LPMOs [which were all expressed heterologously (see below)].

Recently, EPR studies of an AA9-type LPMO active on cellulose (*Ta*AA9A, CAZy abbreviation) and an AA10-type LPMO with strong affinity for chitin (*Ba*AA10A, CAZy abbreviation) have revealed differences in the electronic structures of their copper binding sites.[4,21] The AA9-type LPMO displayed a typical type 2 copper EPR signal based on the Peisach−Blumberg classifications of type 1 and 2 copper enzymes. The EPR signal for *Ba*AA10A indicated an intermediate between type 1 and type 2 copper protein centers. On the basis of the overall axial envelope of the EPR spectrum, it was concluded that a type 2 classification is appropriate for members of the AA10 family; the deviation from standard values (and from members of the AA9 family) was ascribed to a distorted coordination geometry, which indeed is visible in available crystal structures.[21] Notably, *Ba*AA10A probably oxidizes C1 in chitin (there are in fact no activity data for this enzyme), whereas *Ta*AA9A oxidizes both C1 and C4 or C6 in cellulose (Quinlan et al.,[4] whether the enzyme oxidizes C4, C6, or both is a matter of debate).

These dissimilarities in the EPR signals could reflect inherent differences that separate LPMOs into two families, AA9 and AA10, but could also relate to differences in substrate specificity, catalytic efficiency, and/or oxidation mode. To address this, we have expressed and analyzed the activity of two AA10-type LPMOs whose oxidative activity had not been described previously, one active on chitin (from *Bacillus licheniformis*, *Bl*AA10A, CAZy abbreviation) and one active on cellulose (E8 from *T. fusca* YX, *Tf*AA10B, CAZy abbreviation). This then allowed us to compare the sequences (mapped on available structures) and EPR spectra of four AA10-type LPMOs, in total, two acting on cellulose and two acting on chitin. The importance of the Phe/Tyr variation close to the copper site mentioned above, which may codetermine differences between members of the AA9 and AA10 families, was addressed by site-directed mutagenesis of Phe219 in one of the cellulose-active AA10 LPMOs, CelS2 (*Sc*AA10C, CAZy abbreviation).

MATERIALS AND METHODS

Cloning, Site-Directed Mutagenesis, and Protein Expression. A DNA fragment encoding CBP21 (residues 1−197) from *S. marcescens* BJL200 (*Sm*AA10A, UniProt entry O83009) was cloned into the pRSET B expression vector (Invitrogen) with its native signal peptide (residues 1−27), as previously described.[19] Full length CelS2 (residues 35−364) from *Streptomyces coelicolor* A3(2) (*Sc*AA10C, UniProt entry Q9RJY2) was cloned into the pET-32 LIC vector (Novagen) as previously described.[3] The N-terminal LPMO domain (residues 35−230) of CelS2, hereafter termed CelS2-N, was amplified from the pET-32 LIC_*cels2* vector and fused into linearized pRSET B using the In-Fusion HD cloning kit (Clontech). The pRSET B vector was precut with restriction endonucleases (BsmI and HindIII) to remove the nucleotides encoding the mature CBP21 protein but preserving its signal sequence for periplasmic expression. The N-terminal LPMO domain (residues 32−225) of E8 from *T. fusca* YX (*Tf*AA10B, UniProt entry Q47PB9), hereafter termed E8-N, was amplified from genomic DNA (ATCC catalog no. BAA-629D-5), as was the LPMO from *B. licheniformis* (*Bl*AA10A, UniProt entry Q62YN7) (residues 32−203) (genomic DNA, ATCC catalog no. 14580D-5). Both of these latter LPMOs were cloned without their natural signal peptide and inserted into the pRSET B expression vector containing the signal sequence of CBP21, as described for CelS2-N above. A general drawing of the constructs and their domains is presented in Figure S1 of the Supporting Information.

The pRSET B_*cels2-n* plasmid was used as a template for site-directed mutagenesis of the conserved phenylalanine residues near the catalytic site. CelS2-N mutants F219A and F219Y were generated using the QuikChange II site-directed mutagenesis kit (Agilent Technologies). After the mutated expression vectors had been verified by DNA sequencing, they were transformed by heat shock into chemically competent One Shot BL21 Star (DE3) cells (Invitrogen).

For protein expression, fresh colonies were inoculated into LB-Amp (Luria broth medium containing 50 μg/mL ampicillin) medium and grown at 30 °C for 20 h at 200 rpm, with the exception of the CBP21-producing strain, which was grown at 37 °C for 16 h. Cells were harvested by centrifugation, and periplasmic fractions were prepared by osmotic shocking.[24] The periplasmic extracts were sterilized by filtration (0.2 μm) and stored at 4 °C prior to protein purification.

Purification and Generation of Apoenzymes. CelS2-N wild type and mutants, E8-N, and *Bl*AA10A were purified using a two-step protocol, starting with an anion exchange chromatography step followed by gel filtration. The periplasmic fraction was adjusted to buffer A [50 mM Tris-HCl (pH 7.5 or 8.5 for the *Bl*AA10A enzyme)] and loaded onto a 5 mL HiTrap DEAE FF column (GE Healthcare) connected to an ÄKTA purifier fast protein liquid chromatography system (GE Healthcare). LPMOs were eluted by applying a linear salt gradient from 100% buffer A [50 mM Tris-HCl (pH 7.5 or 8.5)] to 50% buffer B (buffer A with 1 M NaCl) over 100 min at a flow rate of 3 mL/min (200 min at 4.5 mL/min for *Bl*AA10A). CelS2-N and its mutants and E8-N were eluted at approximately 12% buffer B, whereas *Bl*AA10A eluted at 8% buffer B. The LPMO-containing fractions were pooled and concentrated to <1 mL, using Amicon Ultra centrifugal filters

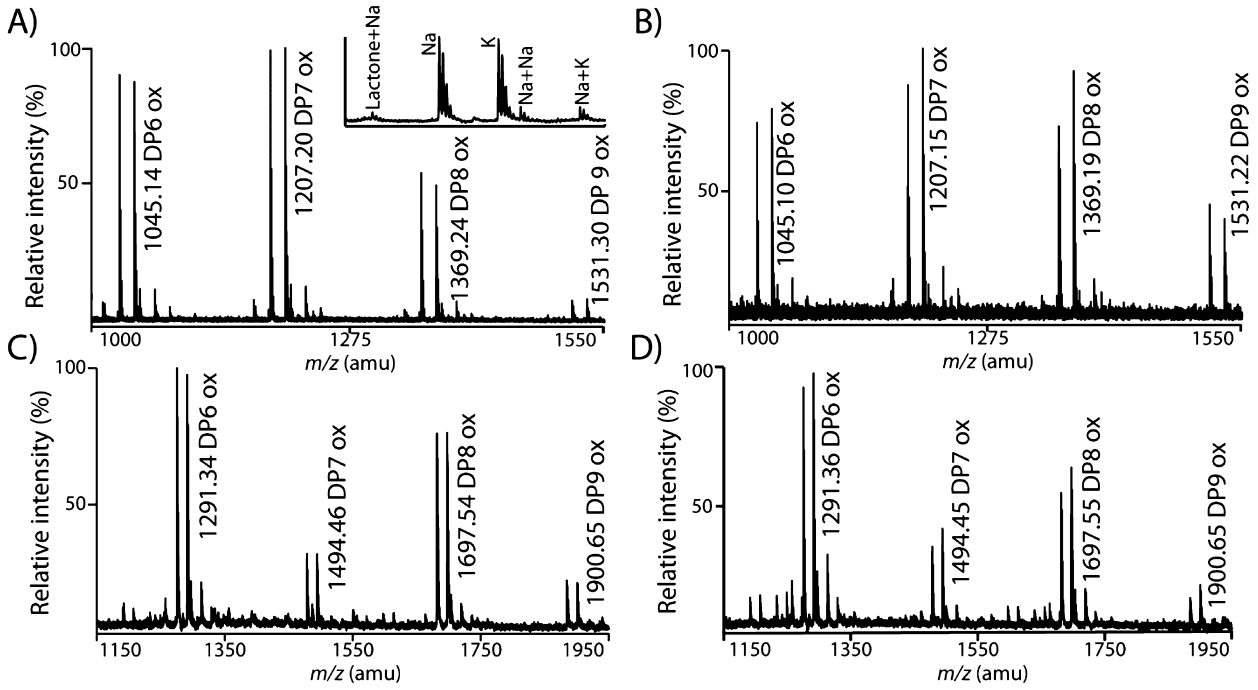

Figure 1. MALDI-TOF MS analysis of LPMO-generated soluble oxidized products. The top two panels show products generated from PASC degradation by CelS2-N (A) and E8-N (B). The bottom two panels show products generated from β-chitin by CBP21 (C) and *Bl*AA10A (D). The annotated masses correspond to the potassium adducts of products in the range from DP6 to DP9 of oxidized cello- or chito-oligosaccharides (Glc_{5-8}Glc1A or $GlcNAc_{5-8}$GlcNAc1A). The sodium adducts, at values m/z 16 lower, yield approximately equally intense signals. The inset in panel A shows the different adducts found in an ionic cluster starting with the sodium adduct of the 1,5 δ-lactone, followed by the sodium and potassium adducts of the aldonic acid, followed by the sodium adducts of the sodium and potassium salts; 100% relative intensity represents 2.2×10^4, 1.5×10^4, 5.6×10^4, and 5.2×10^4 arbitrary units (a.u.) in panels A–D, respectively.

(Millipore) with a molecular mass cutoff of 10000 Da. Subsequently, samples were loaded onto a HiLoad 16/60 Superdex 75 size exclusion column (GE Healthcare), with a running buffer consisting of 50 mM Tris-HCl (pH 7.5) and 200 mM NaCl, using a flow rate of 1 mL/min. All LPMOs eluted approximately 75 min after injection.

CBP21 was purified by chitin affinity chromatography using chitin beads (NEB) equilibrated in 50 mM Tris-HCl (pH 8.0) and 1 M $(NH_4)_2SO_4$ and eluted with 20 mM acetic acid (pH 3.6).[19]

Full length CelS2 from intracellular expression was purified as described previously,[3] using standard immobilized metal affinity chromatography (IMAC) and the nickel-NTA IMAC resin (Qiagen) followed by removal of the His tag using Factor Xa (Novagen). The free His tag and Factor Xa were removed using IMAC chromatography and Xarrest agarose beads (Novagen), respectively.

Protein purity was analyzed by sodium dodecyl sulfate–polyacrylamide gel electrophoresis (SDS–PAGE), and fractions containing pure protein were pooled and concentrated using Amicon filters, followed by a change of buffer to 20 mM Tris-HCl (pH 8.0). Protein concentrations were determined using the Bradford assay (Bio-Rad).

Apo-LPMOs were generated by incubating 100 μM enzyme with 400 μM EDTA in 20 mM Pipes buffer (pH 6.5) for 30 min at room temperature. Subsequently, the buffer was changed to 20 mM Chelex 100 resin (Bio-Rad)-treated Pipes buffer (pH 6.5), until the EDTA concentration was diluted and estimated to be <0.1 nM. The protein concentrations were measured using the Bradford assay.

Product Analysis by MALDI-TOF MS and HPAEC. Products formed after incubation of the Cu(II)-saturated LPMOs with various substrates were analyzed using MALDI-TOF MS. Purified LPMOs at a concentration of 1 μM were incubated with 1 mg/mL substrate (phosphoric acid-swollen cellulose, PASC, prepared from Avicel),[25] squid pen β-chitin (France Chitin, Marseille, France), or shrimp shell α-chitin (Hov Bio, Tromsø, Norway) in 20 mM Bis-Tris buffer (pH 6.0) at 37 °C in the presence of 1 mM ascorbic acid. After incubation for 16 h, the reaction mixtures were centrifuged at 16100*g* for 5 min. Samples from the supernatants were mixed with a 9% solution of 2,5-dihydroxybenzoic acid (DHB) matrix in a 1:2 ratio, after which the samples were air-dried and MALDI-TOF MS analysis was performed as described previously.[2]

For semiquantitative analysis of the activity of CelS2-N wild type and mutants, reactions were set up for each enzyme variant using the conditions described above for PASC degradation. After incubation for 16 h, soluble oxidized products were analyzed by HPAEC using a CarboPac PA1 column and a PAD detector as described by Westereng et al.[26]

Analysis of Substrate Binding by CelS2. One microgram of full length CelS2 or CelS2-N was incubated with an excess of substrate [5–15 mg; filter paper (Whatman #1, 50 μm), dried shrimp shell α-chitin or squid pen β-chitin] in 50 μL of 50 mM Bis-Tris (pH 6.2) at room temperature with slow inversion of the tubes. After 3.5 h, the supernatant was removed by centrifugation and the substrate was washed three times with 500 μL of buffer to remove unspecifically bound enzyme. The bound enzyme was released by denaturing with SDS when boiling the substrates in 50 μL of SDS–PAGE sample buffer for

dx.doi.org/10.1021/bi5000433 | *Biochemistry* 2014, 53, 1647–1656

Table 1. Spin Hamiltonian Parameters[a]

	Cu(II) buffer	CelS2-N[b,c]	E8-N[b]	CBP21	*Bl*AA10A	CelS2-N F219A	CelS2-N F219Y
g_x	2.059	2.015	2.018	2.039	2.038	2.056	2.048
g_y	2.059	2.102	2.103	2.116	2.108	2.058	2.062
g_z	2.270	2.267	2.262	2.260	2.262	2.258	2.248
A_x^{Cu} [d]	12.3	11.7	6.6	42.3	41.3	1.8	23.0
A_y^{Cu} [d]	12.3	17.0	15.3	50.3	48.3	14.0	3.6
A_z^{Cu} [d]	165	153	156	116	125	170	175

[a]Assuming collinear **g** and $\mathbf{A}^{Cu}$ tensors in all simulations. [b]The spectra for CelS2-N and E8-N indicate the presence of free copper, which was corrected by subtracting 30 and 28% of the Cu(II) signal before simulation of the spectra for CelS2-N and E8-N, respectively. [c]The full length CelS2 has EPR parameters identical to those of truncated CelS2-N. [d]Units of $\times 10^{-4}$ cm^{-1}.

10 min. Released proteins, as well as the unbound enzyme fraction and purified enzyme, were then analyzed on an SDS−PAGE gel, using Coomassie Brilliant Blue for staining (Bio-Rad).

Structural Sequence Alignment. PyMod[27] was used to make a structure-based sequence alignment[28] of five AA10-type LPMOs with known structures: *Ef*AA10A (PDB entry 4A02), *Bp*AA10A (PDB entry 3UAM), *Vc*AA10B (PDB entry 2XWX), *Ba*AA10A (PDB entry 2YOX), and CBP21 (PDB entry 2BEM). Chitin activity and binding have been described for all these LPMOs, except for *Bp*AA10A.[19,21,29,30] MUSCLE[31] was then used to add the sequences of the AA10-type LPMOs *Bl*AA10A, *Tf*AA10B, and *Sc*AA10C, which are the subjects of this study.

Electron Paramagnetic Resonance. The EPR spectra were recorded using a BRUKER EleXsyS 560 SuperX instrument equipped with an ER 4122 SHQE SuperX high-sensitivity cavity. Typical settings when recording spectra at 77 K were a microwave power of 0.1−5.0 mW and a modulation amplitude of 10 G (copper quantification purposes) or 30 K a microwave power of 0.5 mW and a modulation amplitude of 5 G when using a liquid helium-cooled Oxford ESR900 cryostat. To estimate the Cu(II) content in the samples, double integrals of baseline-corrected EPR spectra, recorded for the samples and a 100 μM Cu(II) standard in 1 M perchloric acid, were compared.

Apoenzymes were generated as described above and were in Chelex-treated 20 mM Pipes buffer (pH 6.5). EPR studies using the standard conditions described below showed that the apo forms of CelS2-N (enzyme concentration of 108 μM), CBP21 (108 μM), *Bl*AA10A (88 μM), CelS2-N F219A (108 μM), or CelS2-N F219Y (108 μM) did not contain detectable levels of Cu(II). For E8-N (31 μM), approximately 22 μM Cu(II) was detected in the "apoenzyme" (EDTA-treated). Examples of apo-LPMO EPR spectra are shown in Figure S2 of the Supporting Information. Then, Cu(II) was added to the apoenzyme samples to achieve an ∼0.9:1 Cu(II):enzyme ratio. Subsequently, samples were frozen in liquid nitrogen. All Cu(II) added, or initially present and added in the case of E8-N, in the samples could be identified within a margin of error of ∼20%, which is within the expected precision of such analyses. For some of the samples, it was necessary to subtract a fraction of the Cu(II) from the buffer EPR spectrum prior to EPR spectrum simulation (see the simulation parameters listed in Table 1), indicating that not all Cu(II) remained bound to the protein upon the making of the frozen EPR samples. The EasySpin toolbox developed for Matlab was used to simulate and fit EPR spectra.[32]

RESULTS AND DISCUSSION

LPMO Activity Analysis. The four wild-type LPMOs were successfully expressed in *Escherichia coli*. After being purified, stripped of metal ions, and reconstituted with Cu(II), all enzymes showed activity on insoluble polysaccharides [activity measurements on apo-LPMO are not straightforward as it appears that all LPMOs free of metal ions are able to scavenge Cu(II) from the substrate and a large excess of EDTA is required to inhibit oxidation].[4,17,29] The N-terminal LPMO domains of CelS2[3] and E8,[13] called CelS2-N and E8-N, respectively, produced C1-oxidized cello-oligosaccharides from cellulose only (panels A and B of Figure 1, respectively), whereas CBP21[2] and *Bl*AA10A produced C1-oxidized chito-oligosaccharides from α- and β-chitin [panels C and D of Figure 1, respectively (data for α-chitin not shown)], but not from cellulose. To the best of our knowledge, this is the first time that oxidative cleavage of chitin and cellulose is shown for *Bl*AA10A and E8, respectively.

For comparative purposes, full length CelS2 was also produced and purified.[3] Binding studies of CelS2 showed that full length CelS2 binds to filter paper whereas the truncated version, CelS2-N, showed barely detectable binding. For CelS2-N, SDS−PAGE analyses repetitively indicated a minor loss of protein material (compare the filter paper unbound fraction with the control in Figure 2, right panel), which could indicate weak binding, as one would expect considering the detected activity. Remarkably, both full length and truncated CelS2 showed strong binding to both α- and β-chitin. Whereas it is well-known that CBM2s, as present in full length CelS2, bind

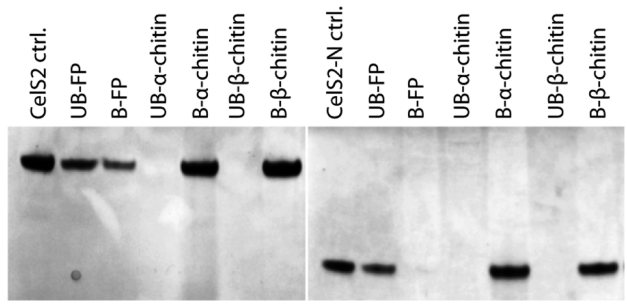

Figure 2. Binding of CelS2 to various substrates. One microgram of full length CelS2 (left) or truncated CelS2-N (right) was incubated with filter paper (FP), α-chitin, or β-chitin for 3.5 h in 20 mM Bis-Tris buffer (pH 6.2) at room temperature. The SDS−PAGE gels document the protein content in the supernatant (unbound, UB) or bound to the substrate (bound, B). The bound protein fraction was released from the substrate by being denatured via boiling in 50 μL of SDS-PAGE sample buffer for 10 min. Purified enzymes were used as a control (ctrl.), not incubated with any substrate, to evaluate protein binding.

dx.doi.org/10.1021/bi5000433 | *Biochemistry* 2014, 53, 1647−1656

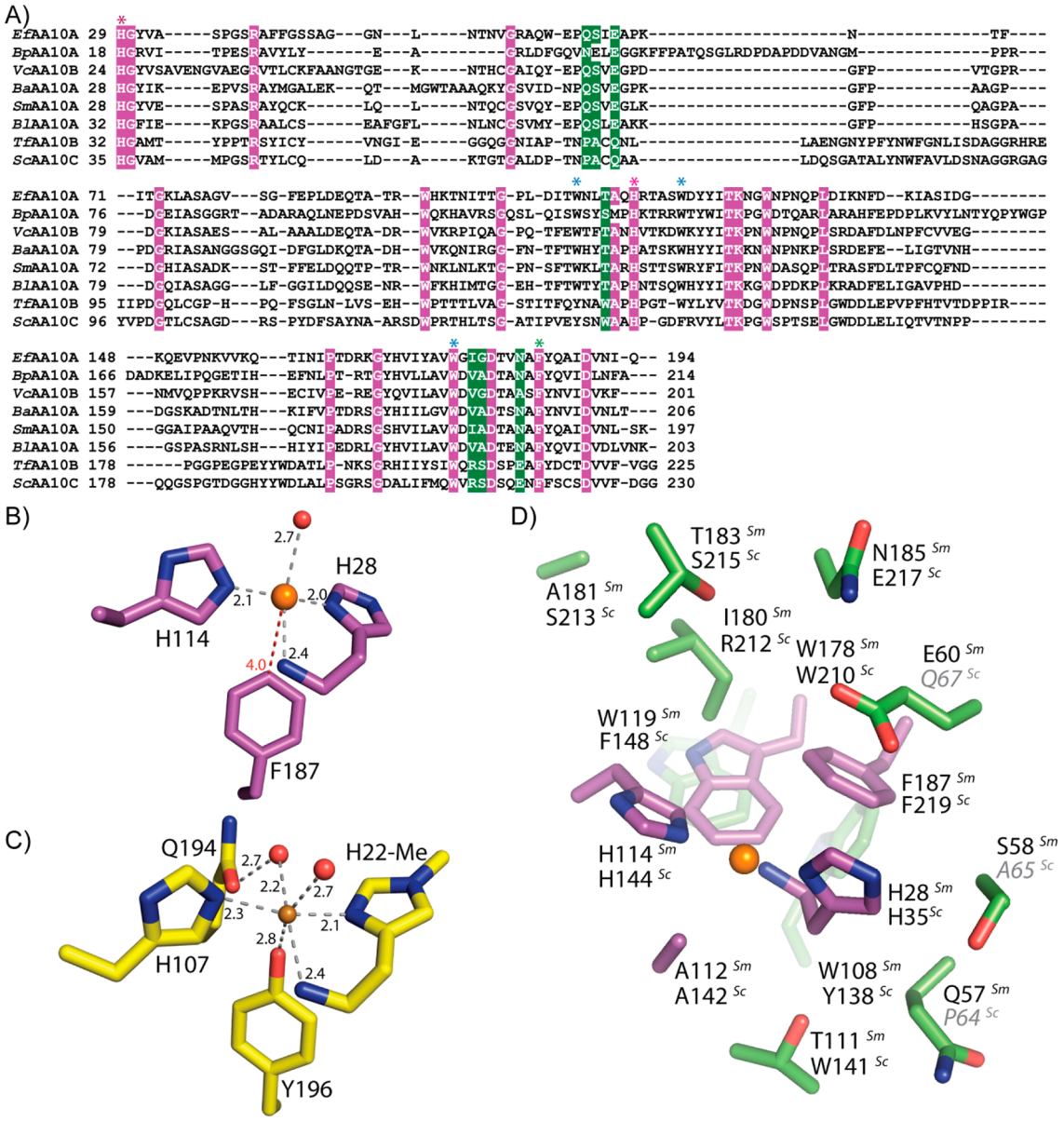

Figure 3. Sequence and structural comparison of LPMO active sites. (A) Structure-based sequence alignment of AA10-type LPMOs. Fully conserved residues are shown with white letters on a pink background; the Cu-coordinating histidines are marked with pink asterisks, and the phenylalanine mutated in CelS2-N (F219A and F219Y) is marked with a green asterisk. The three conserved tryptophans in CBP21 are marked by blue asterisks. Residues highlighted in green are located close to the active site and show variation, potentially determining differences between chitin- and cellulose-active members of the AA10 family (D). (B) Metal coordination in CBP21 representing the AA10-type LPMOs (PDB entry 2BEM).[19] (C) Copper coordination in *Ta*AA9A representing the AA9-type LPMOs (PDB entry 2YET).[4] (D) Expanded view of the active site of CBP21, showing side chains close to the catalytic center that differ between the chitin-active and cellulose-active members of the AA10 family shown in panel A. Pink residues are conserved between all members of the AA10 family in this study, and green residues tend to vary between chitin- and cellulose-active members of the AA10 family. The putative corresponding residues in CelS2 in the unreliable region of the sequence alignment are shown in gray italics. The naming used in the sequence alignment is that from the recommendations of the CAZy database: *Sm*AA10A, CBP21; *Tf*AA10B, E8; *Sc*AA10C, CelS2. Abbreviations in panel D: *Sm*, *Sm*AA10A = CBP21; *Sc*, *Sc*AA10C = CelS2. Figures were made using PyMOL.[38]

to several insoluble polysaccharides, including chitin and cellulose,[33] the strong binding of CelS2-N to α- and β-chitin was unexpected, considering the lack of catalytic activity on these substrates. Upon long incubations (>70 h), we observed barely detectable amounts of soluble products generated from β-chitin by both CelS2-N and E8-N (results not shown). Also, Moser et al.[13] have described experiments indicating that E8 could act synergistically with a chitinase, suggesting some activity on β-chitin. Still, taken together, these results lead to the important conclusion that the ability to bind the substrate and substrate activity and/or specificity are not connected. In other words, the chitin binding demonstrated in Figure 2 is nonproductive. This suggests that other features, such as the geometry of the catalytic center or the character of the redox-active species formed during turnover,[22] could determine which polysaccharides an LPMO can oxidize.

LPMO Sequence Analysis. To provide a structure- and sequence-based basis for interpreting the divergent functions of AA10-type LPMOs, a structure-based alignment of all members of the AA10 family with known structures was made and used

dx.doi.org/10.1021/bi5000433 | *Biochemistry* 2014, 53, 1647−1656

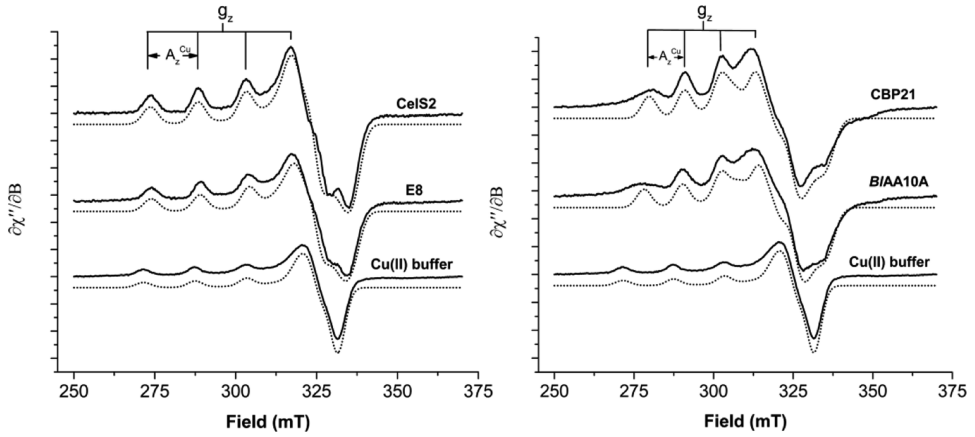

Figure 4. X-Band EPR spectra (—) with simulations (···) for cellulose-oxidizing (left) and chitin-oxidizing (right) AA10-type LPMOs. The superhyperfine splitting occurs at approximately 325 mT. An inset of this for CelS2-N is shown in Figure 6. The spin Hamiltonian parameters in the parallel region are different for chitin- and cellulose-active LPMOs (Table 1). The EPR spectra were recorded at 30 K using a microwave power of 0.5 mW.

to guide alignment of the proteins with unknown structures included in this study (Figure 3A). The level of sequence identity between the cellulose-oxidizing and chitin-oxidizing LPMOs is low (21 and 25% for CelS2-N and CBP21 or *Bl*AA10A, respectively, and 29 and 31% for E8-N and CBP21 or *Bl*AA10A, respectively), whereas the level of sequence identity is ∼50% among LPMOs with the same substrate specificity (46% between the two cellulose-active and 51% between the two chitin-active members of the AA10 family). The metal binding histidines (His28 and His114 in CBP21) are conserved, as are the phenylalanine (Phe187 in CBP21) and the alanine (Ala 112 in CBP21) that are believed to help in shaping the copper binding site in AA10-type LPMOs (Figure 3A,B,D).[21,22]

Notably, several residues close to the copper binding site seem to differ between the cellulose-active and chitin-active LPMOs (Figure 3A,D). A residue that could be important for substrate specificity is Ile180 in CBP21, which is conserved or replaced by Val in other chitin-active members of the AA10 family. This residue lines a pocket on the enzyme surface in the direct proximity of the active site. The two cellulose-active members of the AA10 family contain an arginine at this position.

Another difference between cellulose-active and chitin-active LPMOs that possibly relates to substrate specificity stands out. There are three residues in the N-terminal part of the chitin-active LPMOs, close to the active site (CBP21 residues Gln57, Ser58, and Glu60) that all are solvent-exposed and highly conserved. Because this sequence region is highly diverse (Figure 3A), the sequence alignment is unreliable, and it is thus difficult to predict the corresponding residues in the cellulose-active members of the AA10 family; it is clear though that the sequences vary in this region.

Additional features appearing from this comparison concern the catalytic center itself and the flow of electrons to the copper ion. LPMOs can recruit electrons from a variety of sources, including cellobiose dehydrogenase.[14,15,34] Nothing is known about how electrons are transferred to and through LPMOs. The chitin-active LPMOs contain a fully conserved cluster of three tryptophans that is located directly below the copper binding site (Figure 3D) and that, by analogy to other redox enzymes,[35,36] could play a role in electron transfer.[19,21,22] While the tryptophan residue closest to the metal site (Trp178 in CBP21) is conserved in the two cellulose-active LPMOs, the other two are not (Figure 3A,D). CelS2 has Tyr, Phe, and Trp, whereas E8 has Tyr, Trp, and Trp.

A potentially important difference between the copper binding sites of AA9-type and AA10-type LPMOs concerns the methylation of the N-terminal histidine in the former, a post-transcriptional modification with unknown function. This modification has not been observed in heterologously expressed (and active) LPMOs, including *Phanerochaete chrysosporium* AA9D[37] produced by *Pichia pastoris* and the AA10 LPMOs discussed here, which were all expressed in *E. coli*. To verify the state of the N-terminal histidines in the proteins used for the EPR studies, we analyzed tryptic peptides from recombinantly produced CelS2-N, E8-N, *Bl*AA10A, and CBP21 and found, as expected, that none of the N-terminal tryptic fragments were methylated. Importantly, a similar analysis of CBP21 separated by SDS−PAGE from a culture supernatant of *S. marcescens* grown on chitin did not exhibit methylation of the N-terminal histidine (results not shown).

EPR Spectroscopy. The resting EPR spectra of the Cu(II)-charged AA10 LPMOs showed differences between the two cellulose-degrading enzymes, CelS2-N and E8-N, and the two chitin-degrading enzymes, CBP21 and *Bl*AA10A (Figure 4). The EPR spectra of these enzymes have been simulated, and the estimated spin Hamiltonian parameters are summarized in Table 1. The $\mathbf{g}$ and $\mathbf{A}^{Cu}$ tensors reflect the active site copper coordination environment. The simulations indicated slightly rhombic $\mathbf{g}$ tensors for all enzymes, with CelS2-N and E8-N displaying a higher degree of rhombicity (i.e., a larger difference between g_x and g_y) than CBP21 and *Bl*AA10A. The $g_{x,y}$ and $A_{x,y}^{Cu}$ parameters could not be simulated with the same accuracy as g_z and A_z^{Cu} because the EPR lines in the high-field region are broad and overlap. This is in accordance with what was observed in the work of Hemsworth et al.[21] for *Ba*AA10A, a chitin binding AA10 from *Bacillus amyloliquefaciens*.

By plotting A_z values versus g_z values for several types of copper-containing proteins and model compounds, Peisach and Blumberg observed clear grouping of type 1 and 2 copper proteins.[39] The cellulose-oxidizing *Ta*AA9A (g_z = 2.27, and $A_z^{Cu} = 162 \times 10^{-4}$ cm^{-1})[4] falls nicely into the group of typical type 2 proteins, as do CelS2-N and E8-N (Table 1; g_z and A_z^{Cu} values are very similar to those found for *Ta*AA9A). Interestingly, the A_z^{Cu} hyperfine splitting for the chitin-

dx.doi.org/10.1021/bi5000433 | *Biochemistry* 2014, 53, 1647−1656

oxidizing LPMOs is substantially smaller than for the cellulose-oxidizing LPMOs (Table 1; values of 116 and 125 × 10^{-4} cm^{-1} vs 153 and 156 × 10^{-4} cm^{-1} for the cellulose-active LPMOs). This places the two chitin-oxidizing LPMOs between the usual Peisach−Blumberg type 1 and type 2 classifications. The same was observed for *Ba*AA10A (g_z = 2.25, and A_z^{Cu} = 135 × 10^{-4} cm^{-1}),[21] which has a sequence 49% identical to that of CBP21 (Figure 3A). Hemsworth et al.[21] noted that although *Ba*AA10A falls between the usual Peisach−Blumberg classifications of type 1 and type 2 copper enzymes, the overall axial envelope of the EPR signal would suggest that a type 2 classification is appropriate.[21,39]

Another difference between the cellulose and chitin-active enzymes is that the CelS2-N and E8-N EPR spectra show superhyperfine splitting on the order of 11−16 × 10^{-4} cm^{-1} that is likely to originate from at least two nitrogen atoms coordinating the copper atom (an example is shown for CelS2-N in Figure 4, left). Such superhyperfine splitting is virtually absent from the spectra for the chitin-active LPMOs (Figure 4, right), and this can indicate differences in active site *g* strain and *A* strain. The physical origin of *g* and *A* strain lies in distributions of spin Hamiltonian parameters (i.e., the orientation of the paramagnetic centers) caused by the structural flexibility of the active site. Because cellulose-active LPMOs have less *g* and *A* strain than the chitin-active enzymes, they are more likely to have more structurally defined Cu(II) environments.

It has previously been suggested that the observed differences in the electronic structures of *Ta*AA9A[4] and *Ba*AA10A[21] are due to inherent differences between AA9-type and AA10-type LPMOs.[21] Our data suggest that these previously observed differences are not family-dependent. Instead, they may relate to substrate specificity and/or other aspects of the catalytic features of the enzymes (see below for further discussion).

Site-Directed Mutagenesis of CelS2-N. All four AA10-type LPMOs investigated have a phenylalanine reaching out from the enzyme core toward the copper ion, independent of the substrate preference. While this is a conserved residue in AA10-type LPMOs, it tends to be a tyrosine in AA9-type LPMOs, including *Ta*AA9A [Tyr196 (Figure 3C)], though it should be mentioned that a minor number of members of the AA10 family have a tyrosine and those of the AA9 family have a phenylalanine. To gain insight into the importance of this residue, CelS2-N mutants F219A and F219Y were generated [Phe219 corresponds to Phe187 in CBP21 (shown in Figure 3B)]. The mutants were expressed at levels comparable to that of the wild type and purified in the same way. The activity of the mutants was analyzed by MALDI-TOF MS and HPAEC. The F219Y mutant showed no activity, whereas the F219A mutant showed reduced activity (Figure 5). The amount of soluble products obtained upon PASC degradation suggested that the F219A mutant has a relative activity of approximately 15% compared to that of the wild-type enzyme. These data show that the aromatic ring of Phe219 is not essential for LPMO activity, although it does contribute. It is interesting that the mutation of Phe219 to Tyr, which is present in almost all members of the AA9 family at this position (Figure 3C), was detrimental to activity.

We also investigated copper coordination for the CelS2-N mutants using EPR. The overall EPR envelopes (Figure 6) for the F219 mutants are similar to that of the wild type, with lower g_z and higher A_z^{Cu} values. The data clearly show that the copper site remains intact in both mutants, although with minor

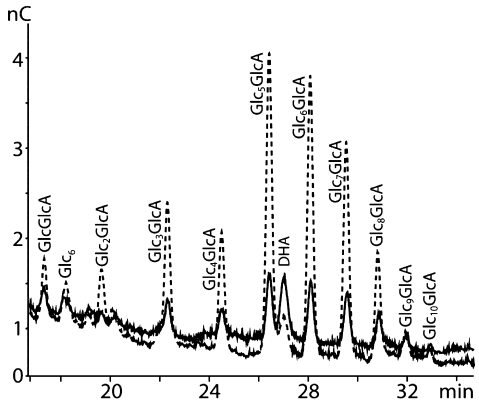

Figure 5. HPAEC chromatograms of oxidized products generated by variants of CelS2-N. Products were analyzed after incubation of CelS2-N wild type or CelS2-N F219A with PASC in 20 mM Bis-Tris (pH 6.0) at 37 °C for 16 h in the presence of 1 mM ascorbate: (···) CelS2-N wild type and (—) CelS2-N F219A mutant. The peak labeled Glc_6 is the result of a cleavage near the reducing end of the polymer. Such sugar moieties will not contain any oxidized functional groups when a C1-oxidizing LPMO interacts with cellulose. Shorter oligomers were also observed prior to the 16 min elution time but were omitted from the figure for the sake of clarity. The peak labeled DHA eluting right after Glc_5GlcA corresponds to dehydroascorbate.

modifications (see values in Table 1). For inactive CelS2-N F219Y, the superhyperfine splitting is even more prominent than for wild-type CelS2-N (Figure 6).

CONCLUDING REMARKS

In this study, we demonstrate the activity of two members of the AA10 family, whose catalytic action has not previously been described, *Bl*AA10A, which oxidizes chitin substrates, and the catalytic LPMO domain of E8 (*Tf*AA10B), which oxidizes cellulose. This allowed us to conduct a comparative study of four AA10-type LPMOs, two acting on chitin and two acting on cellulose.

Substrate binding studies with CelS2 and CelS2-N yielded remarkable results in which both showed strong binding to chitin, on which the enzymes are not active, and weaker and almost no binding to cellulose, on which the enzymes are active. Notably, when LPMO functionality is being assessed, it is important to realize that functional studies normally are conducted with non-natural (i.e., heavily processed) substrates that may be both heterogeneous and structurally dissimilar from "real life". In any case, the data for CelS2 clearly show that differences in the ability to bind certain substrates cannot explain differences in the substrate specificity of catalytic action. All in all, our data suggest that variation in the substrate specificity of LPMOs is determined by the copper active site configuration (because we did observe differences by EPR) and/or the geometry of the enzyme−substrate interaction. Both are conceivably affected by sequence variations directly adjacent to the copper binding site, as discussed above. There are major variations in residues possibly involved in determining substrate specificity (Figure 3D), and there are variations in a cluster of conserved aromatic residues, including Trp178/210 and possibly extending to Phe187/219 (Figure 3D), that may be involved in electron transfer.[21]

The EPR data show that there is considerable variation in the copper-coordinating environments of AA10-type LPMOs. Importantly, the EPR spectra of cellulose-active AA10-type

dx.doi.org/10.1021/bi5000433 | *Biochemistry* 2014, 53, 1647−1656

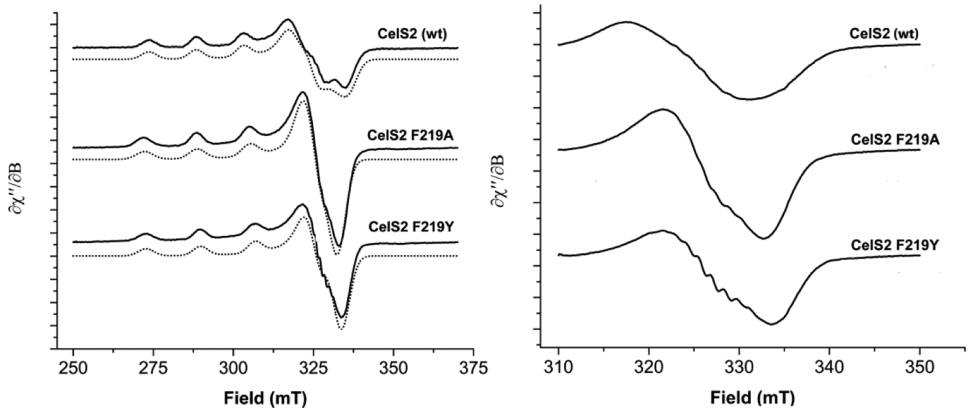

Figure 6. X-Band EPR spectra (—) with simulations (···) for CelS2-N WT, F219A, and F219Y (left). The right panel shows close-ups of the superhyperfine splitting. The EPR spectra were recorded at 30 K using a microwave power of 0.5 mW.

LPMOs are very similar to the EPR spectrum of the cellulose-active AA9-type LPMO *Ta*AA9A,[4] despite the fact that this AA9 enzyme shows some structural differences in or close to the copper binding site. First, the N-terminal copper-coordinating histidine is methylated, which is not the case in the AA10 LPMOs. Second, a conserved Phe in AA10 LPMOs, with its Cζ atom located 4.0 Å from the metal ion in CBP21 (Figure 3B), is replaced by a Tyr in most AA9-type enzymes, with its hydroxyl group 2.8 Å from the metal ion (Figure 3C). The tyrosine residue [Tyr196 in *Ta*AA9A (Figure 3C)] may not be as important as anticipated, because the distance between the tyrosine/tyrosinate in *Ta*AA9A is longer (2.8 Å) than the average 2.38 Å Cu−OTyr bond.[40] Moreover, while mutation of Phe219 to Tyr in CelS2 inactivated the enzyme, the EPR spectrum showed that the copper site remained intact, although with minor modifications. There is no crystal structure for CelS2 or any other cellulose-active AA10 to conclude if there is sufficient space for the added hydroxyl group, which may be the reason why CelS2-N F219Y is inactive. Other mutations (Phe219Ala in this study and Tyr153Phe in *Tt*AA9E described by Harris et al.[9]) indicate that neither the Phe in AA10-type LPMOs nor the Tyr in AA9-type LPMOs is absolutely necessary for activity.

While our data show that there is a correlation between EPR observable variation in the copper binding sites and variation in LPMO functionality, more work needs to be done before the structural basis of LPMO substrate specificity and oxidative power can be unraveled in detail.

As stated by Hemsworth et al.,[21,22] there are clear differences between the active sites of AA10 and AA9. One such difference concerns the steric congestion caused by conserved hydrophobic amino acid sides (Ala112 and Phe187 in CBP21), possibly forcing the substrate to bind solely in the equatorial positions. Our results suggest that the presence of these residues does not determine substrate specificity, which rather seems to be determined by variation at positions that are slightly more remote from the catalytic center. One would certainly expect the structural differences in the copper binding sites themselves to have effects, but these apparently cannot be detected by EPR (or in terms of variation in substrate specificity). Several monomeric copper−oxygen species are known and proposed to be capable of sp^3 carbon oxidation,[22,41] and it is possible that the AA9 and AA10 enzymes differ in terms of how they are generated. Recently, Kim et al. showed, using quantum mechanical calculations, that oxygen binds end-on (η^1) to copper and that a copper-oxyl-mediated oxygen rebound mechanism is energetically preferred on an AA9-type LPMO.[42] It would be interesting to undertake same analyses of the oxygen activation process for members of the AA10 family with varying substrate specificities and compare C1-oxidizing members of the AA9 and AA10 families with similar substrate specificities.

■ ASSOCIATED CONTENT

Supporting Information

A general drawing of the constructs and the domain architecture of LPMOs in this study (Figure S1) and X-band EPR spectra for apo and Cu(II)-charged CelS2 and CBP21 (Figure S2). This material is available free of charge via the Internet at http://pubs.acs.org.

■ AUTHOR INFORMATION

Corresponding Author

*E-mail: morten.sorlie@nmbu.no. Telephone: +47 64965902. Fax: +47 64965901.

Funding

This work was primarily funded by the VISTA program of the Norwegian Academy of Science and Letters, Grant 6505, and by contributions from Norwegian Research Council Projects 196885, 214138, 209335, 218412, and 214239.

Notes

The authors declare no competing financial interest.

■ ACKNOWLEDGMENTS

We thank Morten Skaugen for help with mass spectrometry and Alasdair Mackenzie for help with protein purification.

■ ABBREVIATIONS

AA, auxiliary activities; *Ba*, *B. amyloliquefaciens*; *Bl*, *B. licheniformis*; CBM, carbohydrate binding module; EDTA, ethylenediaminetetraacetic acid; EPR, electron paramagnetic resonance; Glc1A, gluconic acid; GlcNAc1A, gluconic acid of *N*-acetylglucosamine; HPAEC, high-performance anion exchange chromatography; LPMO, lytic polysaccharide monooxygenase; MALDI-TOF MS, matrix-assisted laser desorption ionization time-of-flight mass spectrometry; PASC, phosphoric acid-swollen cellulose; PDB, Protein Data Bank; *Sc*, *S. coelicolor*; *Sm*, *S. marcescens*; *Ta*, *Thermoascus aurantiacus*; *Tf*, *T. fusca*.

REFERENCES

(1) Levasseur, A., Drula, E., Lombard, V., Coutinho, P., and Henrissat, B. (2013) Expansion of the enzymatic repertoire of the CAZy database to integrate auxiliary redox enzymes. *Biotechnol. Biofuels 6*, 41.

(2) Vaaje-Kolstad, G., Westereng, B., Horn, S. J., Liu, Z., Zhai, H., Sørlie, M., and Eijsink, V. G. H. (2010) An oxidative enzyme boosting the enzymatic conversion of recalcitrant polysaccharides. *Science 330*, 219−222.

(3) Forsberg, Z., Vaaje-Kolstad, G., Westereng, B., Bunæs, A. C., Stenstrøm, Y., Mackenzie, A., Sørlie, M., Horn, S. J., and Eijsink, V. G. H. (2011) Cleavage of cellulose by a CBM33 protein. *Protein Sci. 20*, 1479−1483.

(4) Quinlan, R. J., Sweeney, M. D., Lo Leggio, L., Otten, H., Poulsen, J. C., Johansen, K. S., Krogh, K. B., Jorgensen, C. I., Tovborg, M., Anthonsen, A., Tryfona, T., Walter, C. P., Dupree, P., Xu, F., Davies, G. J., and Walton, P. H. (2011) Insights into the oxidative degradation of cellulose by a copper metalloenzyme that exploits biomass components. *Proc. Natl. Acad. Sci. U.S.A. 108*, 15079−15084.

(5) Hemsworth, G. R., Henrissat, B., Davies, G. J., and Walton, P. H. (2014) Discovery and characterization of a new family of lytic polysaccharide monooxygenases. *Nat. Chem. Biol. 10*, 122−126.

(6) Suzuki, K., Suzuki, M., Taiyoji, M., Nikaidou, N., and Watanabe, T. (1998) Chitin binding protein (CBP21) in the culture supernatant of *Serratia marcescens* 2170. *Biosci., Biotechnol., Biochem. 62*, 128−135.

(7) Zeltins, A., and Schrempf, H. (1997) Specific interaction of the *Streptomyces* chitin-binding protein CHB1 with α-chitin: The role of individual tryptophan residues. *Eur. J. Biochem. 246*, 557−564.

(8) Karlsson, J., Saloheimo, M., Siika-aho, M., Tenkanen, M., Penttila, M., and Tjerneld, F. (2001) Homologous expression and characterization of Cel61A (EG IV) of *Trichoderma reesei*. *Eur. J. Biochem. 268*, 6498−6507.

(9) Harris, P. V., Welner, D., McFarland, K. C., Re, E., Navarro Poulsen, J. C., Brown, K., Salbo, R., Ding, H., Vlasenko, E., Merino, S., Xu, F., Cherry, J., Larsen, S., and Lo Leggio, L. (2010) Stimulation of lignocellulosic biomass hydrolysis by proteins of glycoside hydrolase family 61: Structure and function of a large, enigmatic family. *Biochemistry 49*, 3305−3316.

(10) Adav, S. S., Ng, C. S., Arulmani, M., and Sze, S. K. (2010) Quantitative iTRAQ Secretome Analysis of Cellulolytic *Thermobifida fusca*. *J. Proteome Res. 9*, 3016−3024.

(11) Takasuka, T. E., Book, A. J., Lewin, G. R., Currie, C. R., and Fox, B. G. (2013) Aerobic deconstruction of cellulosic biomass by an insect-associated *Streptomyces*. *Sci. Rep. 3*, 1030.

(12) Vaaje-Kolstad, G., Horn, S. J., van Aalten, D. M. F., Synstad, B., and Eijsink, V. G. H. (2005) The Non-catalytic Chitin-binding Protein CBP21 from *Serratia marcescens* Is Essential for Chitin Degradation. *J. Biol. Chem. 280*, 28492−28497.

(13) Moser, F., Irwin, D., Chen, S. L., and Wilson, D. B. (2008) Regulation and characterization of *Thermobifida fusca* carbohydrate-binding module proteins E7 and E8. *Biotechnol. Bioeng. 100*, 1066−1077.

(14) Langston, J. A., Shaghasi, T., Abbate, E., Xu, F., Vlasenko, E., and Sweeney, M. D. (2011) Oxidoreductive cellulose depolymerization by the enzymes cellobiose dehydrogenase and glycoside hydrolase 61. *Appl. Environ. Microbiol. 77*, 7007−7015.

(15) Phillips, C. M., Beeson, W. T., Cate, J. H., and Marletta, M. A. (2011) Cellobiose dehydrogenase and a copper-dependent polysaccharide monooxygenase potentiate cellulose degradation by *Neurospora crassa*. *ACS Chem. Biol. 6*, 1399−1406.

(16) Westereng, B., Ishida, T., Vaaje-Kolstad, G., Wu, M., Eijsink, V. G. H., Igarashi, K., Samejima, M., Ståhlberg, J., Horn, S. J., and Sandgren, M. (2011) The putative endoglucanase PcGH61D from *Phanerochaete chrysosporium* is a metal-dependent oxidative enzyme that cleaves cellulose. *PLoS One 6*, e27807.

(17) Aachmann, F. L., Sørlie, M., Skjåk-Bræk, G., Eijsink, V. G. H., and Vaaje-Kolstad, G. (2012) NMR structure of a lytic polysaccharide monooxygenase provides insight into copper binding, protein dynamics, and substrate interactions. *Proc. Natl. Acad. Sci. U.S.A. 109*, 18779−18784.

(18) Beeson, W. T., Phillips, C. M., Cate, J. H., and Marletta, M. A. (2012) Oxidative cleavage of cellulose by fungal copper-dependent polysaccharide monooxygenases. *J. Am. Chem. Soc. 134*, 890−892.

(19) Vaaje-Kolstad, G., Houston, D. R., Riemen, A. H., Eijsink, V. G. H., and van Aalten, D. M. (2005) Crystal structure and binding properties of the *Serratia marcescens* chitin-binding protein CBP21. *J. Biol. Chem. 280*, 11313−11319.

(20) Karkehabadi, S., Hansson, H., Kim, S., Piens, K., Mitchinson, C., and Sandgren, M. (2008) The first structure of a glycoside hydrolase family 61 member, Cel61B from *Hypocrea jecorina*, at 1.6 Å resolution. *J. Mol. Biol. 383*, 144−154.

(21) Hemsworth, G. R., Taylor, E. J., Kim, R. Q., Gregory, R. C., Lewis, S. J., Turkenburg, J. P., Parkin, A., Davies, G. J., and Walton, P. H. (2013) The Copper Active Site of CBM33 Polysaccharide Oxygenases. *J. Am. Chem. Soc. 135*, 6069−6077.

(22) Hemsworth, G. R., Davies, G. J., and Walton, P. H. (2013) Recent insights into copper-containing lytic polysaccharide mono-oxygenases. *Curr. Opin. Struct. Biol. 23*, 660−668.

(23) Li, X., Beeson, W. T., IV, Phillips, C. M., Marletta, M. A., and Cate, J. H. (2012) Structural basis for substrate targeting and catalysis by fungal polysaccharide monooxygenases. *Structure 20*, 1051−1061.

(24) Manoil, C., and Beckwith, J. (1986) A Genetic Approach to Analyzing Membrane-Protein Topology. *Science 233*, 1403−1408.

(25) Wood, T. M. (1988) Preparation of Crystalline, Amorphous, and Dyed Cellulase Substrates. *Methods Enzymol. 160*, 19−25.

(26) Westereng, B., Agger, J. W., Horn, S. J., Vaaje-Kolstad, G., Aachmann, F. L., Stenstrøm, Y. H., and Eijsink, V. G. H. (2013) Efficient separation of oxidized cello-oligosaccharides generated by cellulose degrading lytic polysaccharide monooxygenases. *J. Chromatogr., A 1271*, 144−152.

(27) Bramucci, E., Paiardini, A., Bossa, F., and Pascarella, S. (2012) PyMod: Sequence similarity searches, multiple sequence-structure alignments, and homology modeling within PyMOL. *BMC Bioinf. 13* (Suppl. 4), S2.

(28) Shindyalov, I. N., and Bourne, P. E. (1998) Protein structure alignment by incremental combinatorial extension (CE) of the optimal path. *Protein Eng. 11*, 739−747.

(29) Vaaje-Kolstad, G., Bøhle, L. A., Gåseidnes, S., Dalhus, B., Bjørås, M., Mathiesen, G., and Eijsink, V. G. H. (2012) Characterization of the chitinolytic machinery of *Enterococcus faecalis* V583 and high-resolution structure of its oxidative CBM33 enzyme. *J. Mol. Biol. 416*, 239−254.

(30) Wong, E., Vaaje-Kolstad, G., Ghosh, A., Hurtado-Guerrero, R., Konarev, P. V., Ibrahim, A. F. M., Svergun, D. I., Eijsink, V. G. H., Chatterjee, N. S., and van Aalten, D. M. F. (2012) The *Vibrio cholerae* Colonization Factor GbpA Possesses a Modular Structure that Governs Binding to Different Host Surfaces. *PLoS Pathog. 8*, e1002373.

(31) Edgar, R. C. (2004) MUSCLE: Multiple sequence alignment with high accuracy and high throughput. *Nucleic Acids Res. 32*, 1792−1797.

(32) Stoll, S., and Schweiger, A. (2006) EasySpin, a comprehensive software package for spectral simulation and analysis in EPR. *J. Magn. Reson. 178*, 42−55.

(33) Boraston, A. B., Bolam, D. N., Gilbert, H. J., and Davies, G. J. (2004) Carbohydrate-binding modules: Fine-tuning polysaccharide recognition. *Biochem. J. 382*, 769−781.

(34) Horn, S. J., Vaaje-Kolstad, G., Westereng, B., and Eijsink, V. G. H. (2012) Novel enzymes for the degradation of cellulose. *Biotechnol. Biofuels 5*, 45.

(35) Gray, H. B., and Winkler, J. R. (2005) Long-range electron transfer. *Proc. Natl. Acad. Sci. U.S.A. 102*, 3534−3539.

(36) Gray, H. B., and Winkler, J. R. (2010) Electron flow through metalloproteins. *Biochim. Biophys. Acta 1797*, 1563−1572.

(37) Wu, M., Beckham, G. T., Larsson, A. M., Ishida, T., Kim, S., Payne, C. M., Himmel, M. E., Crowley, M. F., Horn, S. J., Westereng, B., Igarashi, K., Samejima, M., Ståhlberg, J., Eijsink, V. G. H., and

Sandgren, M. (2013) Crystal structure and computational characterization of the lytic polysaccharide monooxygenase GH61D from the Basidiomycota fungus *Phanerochaete chrysosporium*. *J. Biol. Chem. 288*, 12828−12839.
(38) DeLano, W. L., and Lam, J. W. (2005) PyMOL: A communications tool for computational models. *Abstracts of Papers of the American Chemical Society 230*, U1371−U1372.
(39) Peisach, J., and Blumberg, W. E. (1974) Structural implications derived from the analysis of electron paramagnetic resonance spectra of natural and artificial copper proteins. *Arch. Biochem. Biophys. 165*, 691−708.
(40) Abriata, L. A. (2012) Analysis of copper-ligand bond lengths in X-ray structures of different types of copper sites in proteins. *Acta Crystallogr. D68*, 1223−1231.
(41) Himes, R. A., and Karlin, K. D. (2009) Copper-dioxygen complex mediated C-H bond oxygenation: Relevance for particulate methane monooxygenase (pMMO). *Curr. Opin. Chem. Biol. 13*, 119−131.
(42) Kim, S., Ståhlberg, J., Sandgren, M., Paton, R. S., and Beckham, G. T. (2014) Quantum mechanical calculations suggest that lytic polysaccharide monooxygenases use a copper-oxyl, oxygen-rebound mechanism. *Proc. Natl. Acad. Sci. U.S.A. 111*, 149−154.